Aperture alignment in autocollimator-based deflectometric profilometers

R.D. Geckeler[1], N.A. Artemiev[1], S.K. Barber[2], A. Just[1], I. Lacey[2], O. Kranz[1], B.V. Smith[3], and V.V. Yashchuk[2]

[1] Physikalisch-Technische Bundesanstalt, Bundesallee 100, 38116 Braunschweig, Germany

[2] Lawrence Berkeley National Laboratory, Advanced Light Source, 1 Cyclotron Road, Berkeley, CA 94720, USA

[3] Lawrence Berkeley National Laboratory, Engineering Division, 1 Cyclotron Road, Berkeley, CA 94720, USA

Email: Ralf.Geckeler@ptb.de

Abstract. During the last ten years, deflectometric profilometers have become indispensible tools for the precision form measurement of optical surfaces. They have proven to be especially suitable for characterising beam-shaping optical surfaces for x-ray beamline applications at synchrotrons and Free Electron Lasers. Deflectometric profilometers use surface slope (angle) to assess topography and utilise commercial autocollimators for the contactless slope measurement. To this purpose, the autocollimator beam is deflected by a movable optical square (or pentaprism) towards the surface where a co-moving aperture limits and defines the beam footprint. In this paper, we focus on the precise and reproducible alignment of the aperture relative to the autocollimator's optical axis. Its alignment needs to be maintained while it is scanned across the surface under test. The reproducibility of the autocollimator's measuring conditions during calibration and during its use in the profilometer is of crucial importance to providing precise and traceable angle metrology. In the first part of the paper, we present the aperture alignment procedure developed at the Advanced Light Source, Lawrence Berkeley National Laboratory, USA, for use with their deflectometric profilometers. In the second part, we investigate the topic further by providing extensive ray tracing simulations and calibrations of a commercial autocollimator performed at the Physikalisch-Technische Bundesanstalt, Germany, for evaluating the effects of the positioning of the aperture on the autocollimator's angle response. The investigations which we performed are crucial for reaching fundamental metrological limits in deflectometric profilometry.

Keywords: Deflectometry, profilometry, x-ray optics, synchrotron metrology, autocollimator, alignment, calibration, surface slope metrology

[1] This research was performed while N. A. Artemiev was at Lawrence Berkeley National Laboratory, Advanced Light Source, 1 Cyclotron Road, Berkeley, CA 94720, USA.

[2] This research was performed while I. Lacey was at Lawrence Berkeley National Laboratory, Advanced Light Source, 1 Cyclotron Road, Berkeley, CA 94720, USA.

1. Introduction

The precision form measurement of optical surfaces has been greatly advanced by the development of deflectometric profilometers which use surface slope (angle) to assess topography. They are capable of measuring surfaces which, due to size, as well as topography range and gradient, pose a challenge to classical interferometry. Because of these advantages, deflectometry has turned out to be especially suitable for characterising beam-shaping optical surfaces for x-ray beamline applications at the modern synchrotrons and Free Electron Lasers (FEL), e.g. [1-8]. Due to their large size (up to 1.5 m length), aspherical, rotationally asymmetric shape, and extremely stringent demands on their form accuracy (< 1 nm peak-to-valley in form, < 50 nrad root-mean-squared in slope [9, 10, 11]), they pose equally stringent demands on the quality, alignment, and characterisation of the components of deflectometric devices used for their measurement.

Fig. 1 presents the basic set-up of a deflectometric profilometer, using the Developmental Long Trace Profiler (DLTP) [5, 12] available at the Advanced Light Source (ALS) X-Ray Optics Laboratory (XROL) [13, 14] as an example. (Note that the current DLTP arrangement depicted here is a reversed version of the set-up described in [5].) To assess the local slope (tilt angle) of the surface under test (SUT), the beam of an angle-measuring device is deflected by a movable optical square (pentaprism) towards the SUT, where an aperture limits the beam footprint. Both the optical square and the aperture are moved together to scan the beam along a trace on the SUT. Commercial electronic autocollimators (AC) [15] are capable of providing precise and traceable angle metrology for this purpose. For a comprehensive overview of the usage of autocollimators in deflectometric profilometers and the specific challenges associated with this application, see [16].

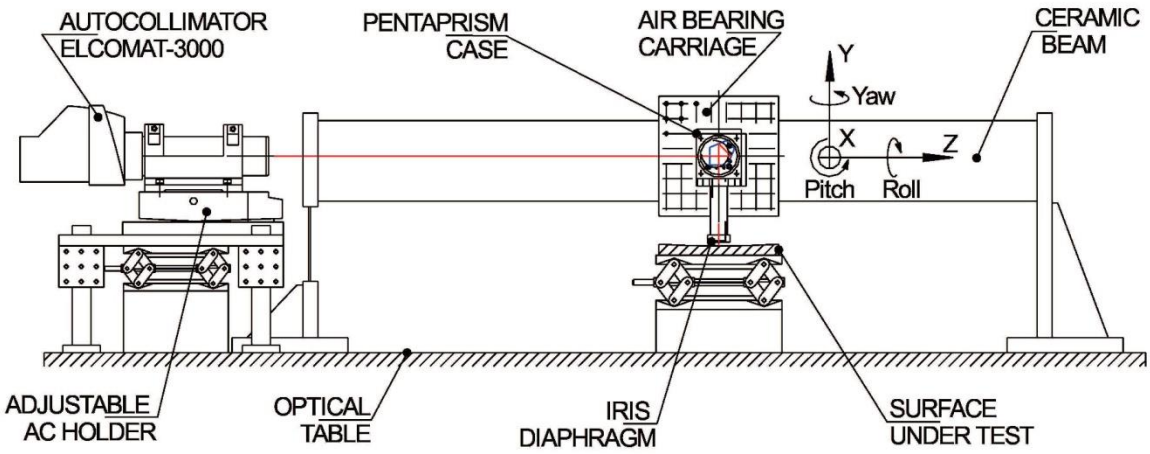

Figure 1. Schematic of a deflectometric profilometer, the Advanced Light Source (ALS) Developmental Long Trace Profiler (DLTP) available at the ALS X-Ray Optics Laboratory (XROL).

After being reflected by the SUT, the returning beam generally follows different geometric paths through the optical components of the profilometer (autocollimator, optical square, and aperture stop) and thus is affected by their aberrations and alignment errors, leading to systematic errors in the autocollimator's angle measurements. For approaching fundamental metrological limits in the deflectometric form measurement, it is essential to reduce the optical aberrations of the profilometer's components and to align them precisely, both relative to each other and internally.

These issues are aggravated by the strong dependence of the systematic errors on the optical path length of the autocollimator's light beam that can change by 1-2 meters when scanning along the SUT [17, 18]. A number of approaches have been proposed to tackle this problem. One example is

the method based on the Universal Test Mirror (UTM) [19] which is directed at revealing the systematic error in deflectometric measurements through a specific experimental arrangement. New calibration devices, such as the Spatial Angle Autocollimator Calibrator (SACC) [20], were developed to accurately calibrate autocollimators over the extended range of application parameters. Modified deflectometric scanning schemes [6] have been suggested which avoid path-dependent angle measurement errors. With all of these methods, the proper alignment of all components of deflectometric profilometers remains of prime importance in order to reduce systematic errors and to use the calibration data for correcting them properly. The need for high lateral resolution in deflectometric profilometry is driving autocollimator apertures towards ever smaller diameters which further increases the demands placed on the alignment of the optical components and on the calibration of the autocollimator.

In a number of publications [12, 21, 22], we extensively treated the alignment of the optical square, including mirror-based pentaprisms. In the cited papers, we provided strategies necessary for the in-situ alignment of the optical square, including its optical faces, the angle measuring axes of the autocollimator, and the SUT, relative to each other. The developed methods have advanced the state-of-the-art to a level at which the error influence of the optical square on form measurement becomes negligible.

In this paper, we focus on one more important issue which has so far been neglected in the literature: the precise and reproducible alignment of the aperture relative to the autocollimator's optical axis. The importance of this task has been recognized by its inclusion in the European Metrology Research Programme (EMRP) SIB 58 Angle Metrology [23]. One topic is the development of a device and a standardised procedure for the positioning of small (1.5-2.5 mm) apertures relative to the autocollimator's optical axis with reproducibility < 0.1 mm. In Section 2, we present the aperture alignment procedure developed at the Advanced Light Source (ALS), Lawrence Berkeley National Laboratory, USA, for use with their DLTP [5, 12]. In Section 3, we present results of ray tracing simulations of a commercial autocollimator at the Physikalisch-Technische Bundesanstalt (PTB) for evaluating the effects of the positioning of the aperture on the autocollimator's angle response. In Section 3, we corroborate the procedures and ray tracing results from the preceding sections by means of autocollimator calibrations performed at the PTB.

2. Aperture alignment with the ALS DLTP

In this section, we describe an experimental method for the precise and reproducible alignment of the beam limiting aperture with respect to the optical axis of the autocollimator in the ALS DLTP [5, 12]. The ALS DLTP is a classical deflectometer based on a movable pentaprism and an electronic AC Elcomat-3000/8 in an arrangement schematically shown in Fig. 1. The strength of the method is that it relies on the propagation of the autocollimator's measuring beam itself which also serves as a natural straightness standard in deflectometric profilometers. As this is a natural choice, there are some similarities to approaches developed at other places [24].

To extend the slope variation measurements into the short spatial wavelength region, a beam limiting aperture (iris diaphragm) of 2.5 mm diameter is used. This is the recommended smallest size of the aperture through which the autocollimator is able to perform reliable angular measurements. The aperture is mounted on an X-Y translation stage (Thorlabs model LM1XY) and attached to the aperture mount of the mirror based pentaprism assembly (Fig. 2). The X-Y stage is used to align the aperture with respect to the AC optical axis.

The optical head of the DLTP (including the pentaprism and the aperture) is placed on an air-bearing movable carriage. Note that in the current version of the DLTP, there are two replaceable optical heads, one for measurements with face up (it is shown in Fig. 2) and other with side facing SUTs.

The aperture alignment procedure consists of of a few steps.

First, the AC optical axis is aligned to be collinear with the axis of translation of the carriage. For this, the AC beam is apertured with a pinhole mounted in the center of the autocollimator output light beam. Practically, a plastic cap with an approximately 1 mm hole in the center is attached to the autocollimator lens tube (Fig. 2). The position of the apertured AC beam is monitored with a CCD camera (IPX-4M15-L) placed on the carriage in the front of the pentaprism assembly. The cross-section of the apertured beam has characteristic cross-like shape shown in Fig. 3 as imaged with the camera placed at a distance of approximately 470 mm from the autocollimator. The high resolution and large field of view of the camera with 2048 × 2048 pixels of 7.4 µm × 7.4 µm size allow visual positioning of the center of the cross-like beam with sub 0.1-mm accuracy. The collinearity of the AC optical axis and the carriage translation axis is adjusted by tilting the autocollimator with a dedicated kinematic stage to minimize the variation of the aperture beam position when translating the carriage over the entire translation range of about 1 m.

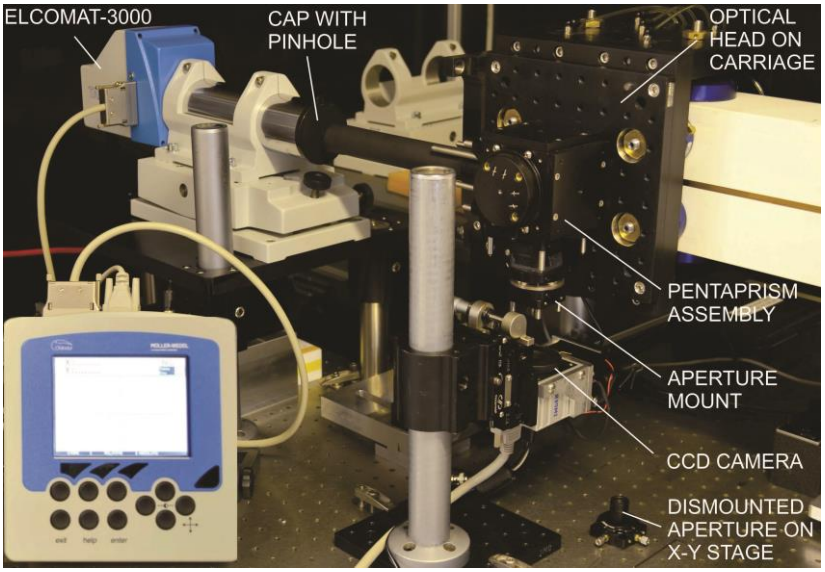

Figure 2. DLTP experimental arrangement for alignment of the DLTP beam limiting aperture. A plastic cap with a 1 mm pinhole is attached to the autocollimator optical tube. The CCD camera is shown in the position used for alignment of the beam limiting aperture of the optical head designed for measurements with face up SUTs. In order to adjust collinearity of the AC optical axis and the carriage translation axis, the camera is mounted in the front of the pentaprism assembly. In the latter arrangement of the camera, it is easy to verify the coincidence of the pinhole center with the optical axis of the autocollimator by rotating the pinhole cap in place and checking that the image of the apertured beam stays unmoved.

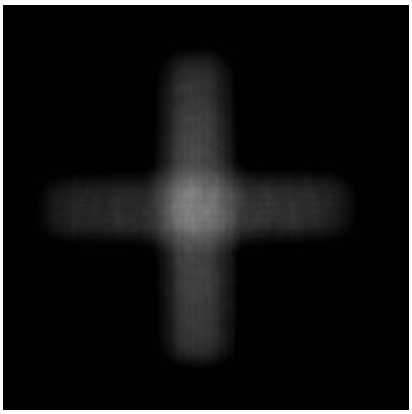

Figure 3. A typical image of the autocollimator light beam apertured with the 1-mm pinhole and recorded with the CCD camera. Distance between the pinhole and the CCD is approximately 470 mm. The recorded field of view is 15 mm × 15 mm.

When the collinearity is adjusted, the CCD camera is removed from the carriage and mounted on the optical table in the position of the SUT in Fig. 1. This arrangement, depicted in Fig. 2, is suitable for recording the AC apertured beam after it passes through the DLTP pentaprism and the beam limiting aperture (iris diaphragm) at a certain fixed position of the carriage.This allows to achieve the alignment goal on this step that is to center the iris diaphragm with respect to the apertured beam.

Starting with the iris diaphragm removed, an image of the cross-shaped beam is recorded in order to accurately determine its center. To simplify the positioning of the beam center, we use specially developed LabView™-based software for the camera control and image acquisition and analysis. However, sub 0.2-mm accuracy of the positioning is easily achievable with manual centering of a marker shown with the green square in Fig. 4. If higher accuracy is desired, a more sophisticated procedure can be implemented, e.g., calculating the centroid of the beam intensity distribution.

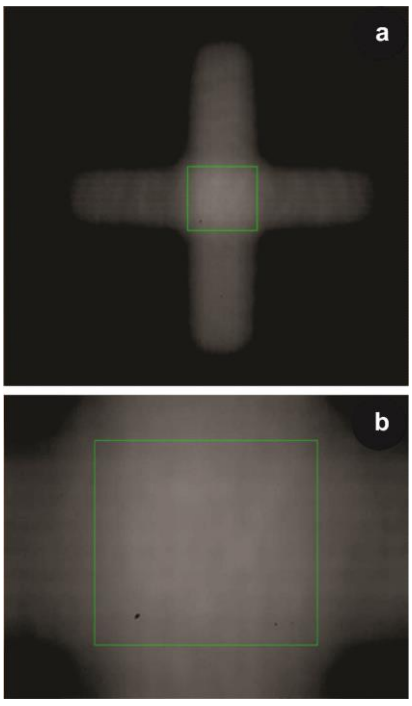

Figure 4. Illustration of the procedure for positioning of the center of the autocollimator cross-like

light beam with a green colored square marker: a) the beam intensity distribution recorded over the whole camera field-of-view; b) the enlarged central part of beam image used to increase the accuracy of the manual positioning.

Next, the iris diaphragm is mounted back on the X-Y translation stage which is part of the DLTP optical head and located right after the pentaprism (see also Fig. 1). With the stage, manual positioning of the aperture in the plane perpendicular to the autocollimator beam is provided. Fig. 5 shows the images of the intensity distribution of the autocollimator light beam in Fig. 4 but limited by the aperture orifice. The optimal positioning consists of matching the orifice center to the center of the cross-like beam depicted in the images with the green square marker. Note that the images may also be used for the precise setting of the aperture size when an adjustable aperture (e.g., iris diaphragm) is used.

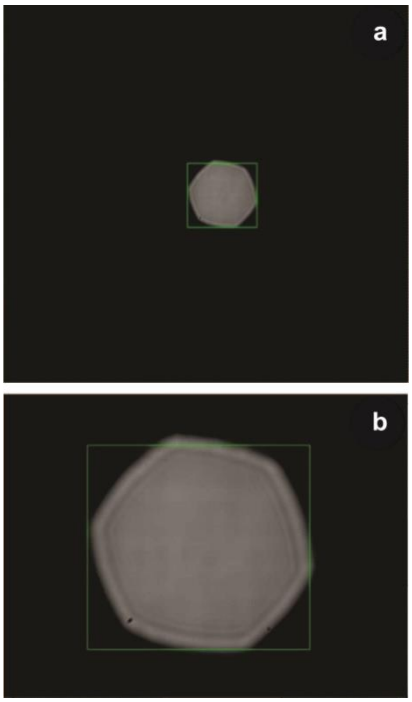

Figure 5. Illustration of matching the orifice center to the center of the autocollimator depicted with the green square marker: a) the beam intensity distribution limited with the aperture and recorded over the whole camera field-of-view; b) the enlarged central part of the beam image used to increase the accuracy of the matching.

So far we assumed that the profiler's pentaprism is optimally aligned with respect to the AC optical axis. In the case of the DLTP, where the pentaprism is made of two mirrors, a special alignment procedure has been developed and described in detail in [12, 21]. The procedure for optimal alignment of the pentaprism relies on the appropriate alignment of the profiler's beam limiting aperture. Therefore, alignment of the aperture, described above in this section, generally requires sequential realignment of the pentaprism. For the global optimization of the DLTP optical head, we perform a few iterative optimizations of the aperture position with subsequent realignment of the pentaprism (at the position of the aperture determined in the previous iteration).

Finally, usually after 1-2 iterations, when the mutual alignment of the all DLTP components is fixed, we check that the alignment stays optimal for the entire translation range of the DLTP carriage. The

check is performed at the extreme carriage positions, the closest and the furthest possible ones, separated by approximately 1 m. With the camera placed at each of these extreme positions on the optical table and with the iris diaphragm totally open,, we find the position of the center of the AC apertured cross-like beam (the first step of the beam limiting aperture alignment procedure, described above). After that, with the iris diaphragm set to the desired 2.5-mm diameter, we check the coincidence of its orifice center with the center of the AC beam.

3. Autocollimator ray tracing

Deflectometric profilometry requires the use of an aperture which restricts the footprint of the autocollimator's measuring beam on the SUT, see Fig. 1. As mentioned above, if the position of the aperture relative to the autocollimator's optical axis is changed, both the outgoing and the returning beams (i.e., the illumination and imaging beams, respectively) follow different paths through the autocollimator's optics. In the presence of aberrations of its optical components and errors in their alignment (including that of the CCD detector), angle measuring deviations are an unavoidable outcome. They are sensitive to the aperture's location perpendicular to the optical axis of the autocollimator and *along* it, i.e., the distances to the autocollimator's objective and to the SUT [16, 17].

As mentioned above, in the case of deflectometric profilometers, to access different points on the SUT, the aperture is moved along the autocollimator's optical axis together with the pentaprism. If straightness errors of the linear stage used for moving them are present or if the stage and the autocollimator's optical axis are not parallel, parasitic changes in the aperture's position perpendicular to the optical axis are unavoidable.

3.1. Model for ray tracing

The effect of lateral shifts of the aperture on the autocollimator's angle measurement has been investigated by ray-tracing simulations. To this purpose, a model of an Elcomat-3000/8 [15], which is commonly used for high-precision deflectometric applications, has been created with the optic simulation software ZEMAX. It considers the optical components of this autocollimator type which features two different beam paths for its horizontal and vertical measurement axes with separate illumination units, reticles, and CCD lines, but a common objective. The beam paths and the respective illumination units and CCD lines are divided by beam splitters. The model has been simplified to speed up the simulations (see Fig. 6): The two beam paths have been simulated by a single beam path. Therefore, only one point light source (simulating the illuminations and the reticles) and one plane detector (simulating the CCD lines), located at the same position in the model, were implemented. To retain the original optical path length, two plane-parallel plates simulate the beam splitters.

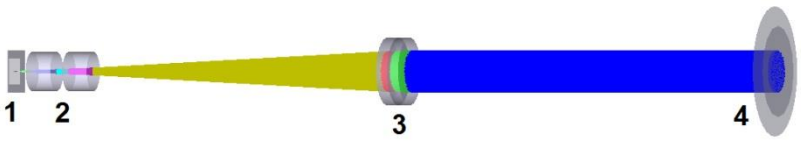

Figure 6. Simplified ZEMAX model of the simulated autocollimator. 1: detector and point light source, located at the objective's focal plane; 2: two plane-parallel plates; 3: objective; 4: aperture (diameter 32 mm in this graph) and SUT, 5 mm apart.

The aperture diameter was set to B=2.5 mm as this a typical value chosen in autocollimator-based

deflectometry. The spacing between the aperture and the SUT was fixed at 5 mm. In the simulations, the SUT was rotated in such a way that only one of the autocollimator's measuring axes was engaged, i.e., the axis which is parallel to the plane of the beam deflection. For the presented simulations, the aperture was decentred from the autocollimator's optical axis in the direction parallel to this axis / plane. The lateral position of the aperture, X, is defined as the distance between the autocollimator's optical axis and the aperture's centre. Note that varying the lateral position of the aperture in the perpendicular direction has no effect on the presented results.

For all investigations, one reference simulation (lateral position of the aperture: X=0 mm, i.e. the aperture is centred on the optical axis of the autocollimator) and several measurement simulations (X=0.5 mm, X=1 mm, X=1.5 mm, and X=2 mm) have been performed. The mirror angles were varied from -1350 arcsec to 1350 arcsec in steps of 54 arcsec. The differences between the measured angles of the measurement simulations and the reference simulation were calculated.

The influence of the lateral aperture position on the angle measurement of the autocollimator has been investigated at distances between the SUT and the autocollimator of D=25 mm, 300 mm, 600 mm, 900 mm, 1200 mm, and 1500 mm. The distances were equal for the reference simulations and the respective measurement simulations with the laterally shifted aperture.

3.2. Simulation results

Fig. 7-10 show the angle measuring deviations caused by lateral shifts of the aperture. The figures present a selection of the simulation results. In Fig. 7-8, the lateral aperture position X was varied, in Fig. 9-10 the distance D was varied.

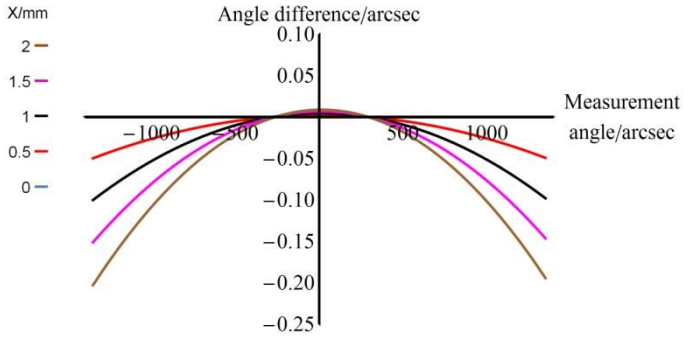

Figure 7. Angle deviations of the autocollimator for different lateral aperture positions X, aperture size B=2.5 mm, and distance D=300 mm.

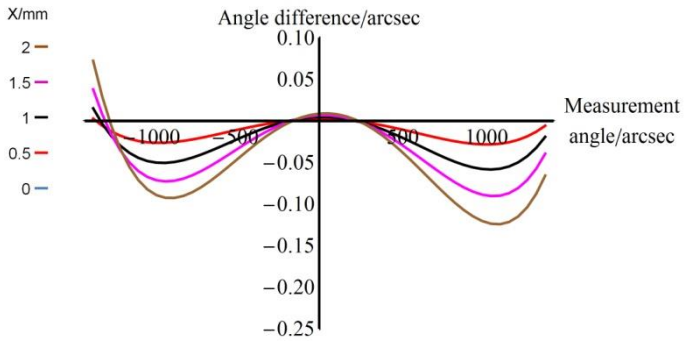

Figure 8. Angle deviations of the autocollimator for different lateral aperture positions X, aperture size B=2.5 mm, and distance D=1500 mm.

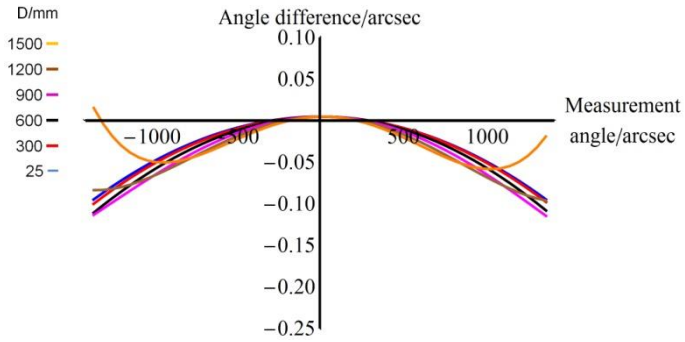

Figure 9. Angle deviations of the autocollimator for different distances D, lateral aperture position X=1 mm, and aperture size B=2.5 mm.

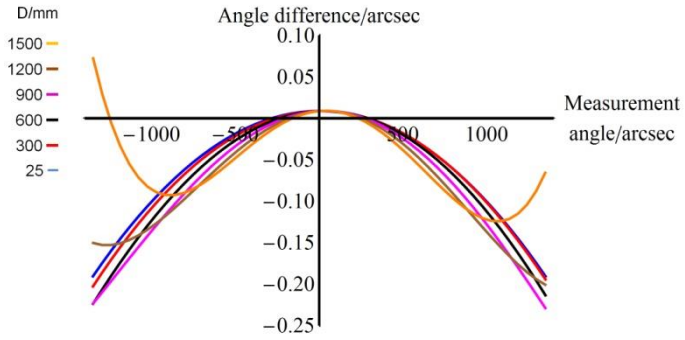

Figure 10. Angle deviations of the autocollimator for different distances D, lateral aperture position X=2 mm, and aperture size B=2.5 mm.

The standard deviations of the angle differences (in arcsec) within the simulated measurement range of -1350 arcsec to 1350 arcsec for the respective lateral aperture positions X and distances D are given in Table 1.

X/mm	D/mm					
	25	300	600	900	1200	1500
0.5	0.016	0.016	0.018	0.019	0.017	0.011
1	0.031	0.033	0.036	0.038	0.033	0.022
1.5	0.047	0.049	0.054	0.057	0.050	0.034
2	0.063	0.065	0.072	0.075	0.066	0.047

Table 1: Standard deviations of the angle differences in arcsec, calculated for the simulated measurement range of -1350 arcsec to 1350 arcsec.

For constant angles of the mirror, the measured angles differ when the aperture is shifted laterally in the direction of the beam deflection even for a SUT angle of $\alpha = 0$. Fig. 11 shows a magnified section

of Fig. 7 to highlight this effect. It necessitates a precise adjustment of the optical axis of the autocollimator with respect to the linear stage (i.e. the movement direction of the aperture).

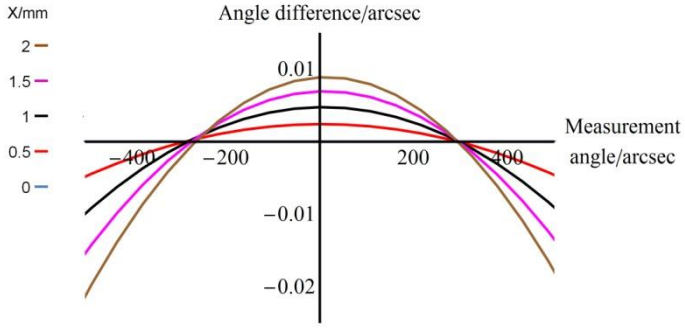

Figure 11. Angle deviations of the autocollimator for different lateral aperture positions X , aperture size B=2.5 mm, and distance D=300 mm in a measurement range of -500 to 500 arcsec. The angle deviation of the autocollimator is not constantly zero for a SUT angle of $\alpha = 0$.

The light source and the detector have been placed at the position of the objective's focal plane which was determined by ZEMAX with an optimization algorithm. The optimisation was performed with a centred full aperture (B=32 mm) in accordance with the manufacturers adjustment procedure. However, the focal plane is different for an aperture with B=2.5 mm. When the aperture is shifted laterally, this causes a displacement of the position of the incident rays on the detector and, therefore, an angle response of the autocollimator for $\alpha = 0$. For an aperture shift of X, the angle deviation of the autocollimator, $\Delta\alpha$, is given by the relation

$$\frac{\Delta\alpha(\mathrm{X}, \alpha = 0)}{1\ \mathrm{arcsec}} \approx 4.45\ \frac{\mathrm{X}}{1\mathrm{m}}$$

The performed simulations show the sensitivity of the angle measurement of the simulated autocollimator with respect to variable lateral shifts of the aperture at different distances. An analysis of the simulations for a distance D=1500 mm, an aperture size B=2.5 mm, and an angle range of ±1350 arcsec, see Fig. 8, indicates that for an aperture centred within X=±0.08 mm, the errors in the autocollimator's angle measurement remain below 50 nrad peak-to-valley.

Notice that the results of the ray-tracing simulations and the derived equations are valid for the simulated autocollimator only.

4. Autocollimator calibration data

Angle measurement with autocollimators is sensitive to the measuring conditions [11, 16, 17, 25]. The factors influencing the angle response of an autocollimator can be sub-divided into two broad categories, internal vs. external.

Internal factors are specific to the each autocollimator's internal design and, therefore, are generally beyond user control. They include aberrations of the optical components (objective, reticle illumination, beam splitter cubes, etc.), their alignment (including that of the CCD detector), the non-orthogonality of the measuring axes, internal specular reflections and stray light, geometrical imperfections of the reticles, *inter*-pixel variations of the CCD (geometry, quantum efficiency, dark current, and more), and *intra*-pixel quantum efficiency patterns (across *single* CCD pixels, due to their internal structure).

External factors are given by the measuring conditions under which the device is used in the set-up

and, therefore, to a certain extent, are subject to control by the user. These include the reflectivity and curvature of the SUT, the path length of the autocollimator beam probing it, the diameter and shape of the aperture stop, and the position of the aperture stop along the autocollimator's optical axis and perpendicular to it.

Traceable autocollimator calibration is central to making full use of their potential by correcting their angle measurement errors and, therefore, is essential for approaching fundamental metrological limits in deflectometric form measurement. At the PTB, autocollimator calibration is realized by its direct comparison to the primary angle standard, the Heidenhain WMT 220 angle comparator, manufactured by Dr. Johannes Heidenhain GmbH, Traunreut, Germany [26]. With the aid of various self- and cross-calibration techniques, the standard measurement uncertainty [27] of the WMT 220 could be reduced to u = 0.001 arcsec (5 nrad) [28, 29]. With highly stable autocollimators, calibrations with standard uncertainties down to u = 0.003 arcsec (15 nrad) [11, 16, 17, 25] have been achieved. The uncertainty budget for the autocollimator calibration includes components which depend on the type of autocollimator and the calibration parameters. They usually dominate the final uncertainty budget and may result in budgets larger than the one stated above. In contrast, the uncertainty contribution of the primary angle standard WMT 220 is of subordinate importance. Even better autocollimator calibration results have been achieved by the application of a novel error-separating shearing approach [30].

By use of the primary angle standard WMT 220 of PTB we obtained calibration data of an autocollimator type Elcomat 3000, Möller-Wedel Optical [15]. The standard calibration set-up follows the scheme laid out in Fig. 6 with a coated SUT placed at a distance of 300 mm with respect to the front end of the autocollimator's objective. The SUT was coated with Aluminium (resulting in a high reflectivity). A circular aperture 2.5 mm in diameter was placed close (at a distance of 3 mm) to the optical surface of the SUT. The aperture was shifted laterally in the direction of the primary measuring plane, i.e., in the plane of the beam deflection. Displacements of the aperture with respect to the autocollimator's optical axis of 0.75 mm to 5 mm were realised.

Fig. 12 shows the differences between the angle responses of the autocollimator for the selected off-centre locations of the aperture and for a centred aperture. For the selected calibration range of ±1000 arcsec, differences of several tenths of an arcsec are visible. (Note that autocollimators are not designed for use with small apertures and therefore show angle deviations which are much larger than the ones expected when they are used within the parameter range for which their design has been optimised.) These results stress the importance of a reproducible alignment of the aperture during calibration and subsequent use of the autocollimator. A comparison of the results of the ray tracing simulations (Sec. 3) and of the experimental data shows no strong similarities, neither with respect to the course of the differences nor their magnitude. It is our conclusion that the shifting of the aperture makes visible effects which are dominated by the influence of minor manufacturing differences of each individual autocollimator rather than by the influence of its general design. These may include limits in the alignment of the autocollimator's optical components, small-scale inhomogeneities and flatness deviations of the components, as well as inhomogeneities in the pixel response and geometrical layout of the CCD detector, etc. These results furthermore stress the importance of a reproducible aperture alignment.

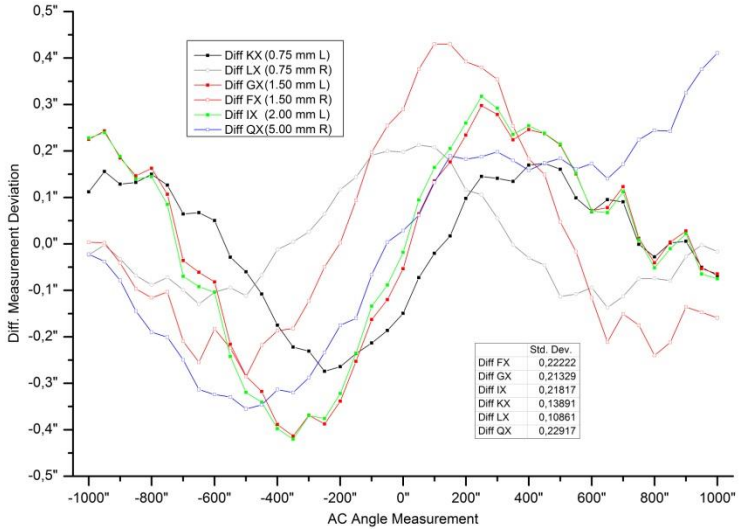

Figure 12. Differences between the angle response of an autocollimator for selected off-centre locations of the aperture and for a centred aperture. The distance of the SUT was 300 mm. The circular aperture, 2.5 mm in diameter, was placed close to the SUT and shifted with respect to the autocollimator's optical axis by 0.75 mm to 5 mm.

5. Conclusions

In deflectometric profilometers, the precise and reproducible alignment of the beam-limiting aperture relative to the autocollimator's optical axis and its maintenance while it is scanned across the surface under test are important for reaching fundamental metrological limits. These requirements aim at creating reproducible measuring conditions for the autocollimator during calibration and during its use in the profilometer to ensure optimal traceability of the angle metrology to national standards. Ultimately, calibration data are only applicable to correcting the autocollimator's angle readings if differences between the measuring conditions remain within tightly specified limits.

In this paper, we demonstrated recent progress in this field. The aperture alignment procedure developed at the ALS provides an approach that allows reproducing - in different experimental arrangements and in different metrology labs - exactly the same alignment of the particular autocollimator and aperture. The described procedure has a potential to be accepted as a standard alignment procedure for autocollimator-based deflectometric profilometers. Its strength is that it relies on the propagation of the autocollimator's measuring beam which serves as a natural straightness standard in deflectometric profilometers.

The ray tracing simulations and calibrations of a commercial autocollimator performed at the PTB demonstrated that additional effort needs to be put into understanding all effects of the displacement of the aperture relative to the autocollimator's optical axis on its angle response. Especially the discrepancy between simulations and calibrations demonstrates that the idealised ray tracing model needs to be augmented by incorporating, e.g., misalignments and imperfections of the autocollimator's optical components. As a result of the ray tracing simulations, we recommend a reproducibility of the aperture alignment within ±0.1 mm.

Acknowledgements

The authors are very grateful to Gary Centers for useful discussions.

Part of this research was undertaken within the EMRP JRP SIB58 *Angle Metrology*. The EMRP is jointly funded by the EMRP participating countries within EURAMET and the European Union.

The Advanced Light Source is supported by the Director, Office of Science, Office of Basic Energy Sciences, Material Science Division, of the U.S. Department of Energy under Contract No. DE-AC02-05CH11231 at Lawrence Berkeley National Laboratory.

References

[1] F. Siewert, J. Buchheim, S. Boutet, G.J. Williams, P.A. Montanez, J. Krzywinski, and R. Signorato, *Opt. Express* **20**(4), 4525 (2012).

[2] G. Ehret, M. Schulz, M Stavridis, and C. Elster, *Meas. Sci. Technol.* **23**, 094007 (2012).

[3] F. Siewert, J. Buchheim, T. Zeschke, G. Brenner, S. Kapitzki, and K. Tiedtke, *Nucl. Instrum. Methods Phys. Res., Sect. A* **635**, 52 (2011).

[4] Z. Ali, N.A. Artemiev, C.L. Cummings, E.E. Domning, N. Kelez, W.R. McKinney, D.J. Merthe, G.Y. Morrison, B.V. Smith, and V.V. Yashchuk, *Proc. SPIE* **8141**, 81410O (2011).

[5] V.V. Yashchuk, S. Barber, E.E. Domning, J.L. Kirschman, G.Y. Morrison, B.V. Smith, F. Siewert, T. Zeschke, R.D. Geckeler, and A. Just, *Nucl. Instrum. Methods Phys. Res., Sect. A* **616**, 212 (2010).

[6] M. Schulz, G. Ehret, and A. Fitzenreiter, *J. Eur. Opt. Soc. Rapid Publications* **5**, 10026 (2010).

[7] J.L. Kirschman, E.E. Domning, W.R. McKinney, G.Y. Morrison, B.V. Smith, and V.V. Yashchuk, *Proc. SPIE* **7077**, 70770A (2008).

[8] F. Siewert, H. Lammert, T. Zeschke, 'The Nanometer Optical Component Measuring Machine' in *Modern Developments in X-ray and Neutron Optics* (Springer, Berlin, Germany, 2008).

[9] D. Mills and H. Padmore, 'X-ray Optics for BES Light Source Facilities' in *Report of the Basic Energy Sciences Workshop on X-ray Optics for BES Light Source Facilities* (U.S. Department of Energy, Office of Science, Potomac, U.S., 2013).

[10] H. Sinn, J. Gaudin, L. Samoylova, A. Trapp, and G. Galasso, 'X-Ray Optics and Beam Transport' (European X-Ray Free-Electron Laser Facility GmbH, Hamburg, Germany, 2011).

[11] L. Samoylova, H. Sinn, F. Siewert, H. Mimura, K. Yamauchi, and T. Tschentscher, *Proc. SPIE* **7360**, 1 (2009).

[12] S.K. Barber, G.Y. Morrison, V.V. Yashchuk, M.V. Gubarev, R.D. Geckeler, J. Buchheim, F. Siewert, and T. Zeschke, *Opt. Eng.* **50**(5), 053601 (2011).

[13] V. V. Yashchuk, N. A. Artemiev, I. Lacey, W. R. McKinney, and H. A. Padmore, *Proc. SPIE Int. Soc. Opt. Eng.* **9206**, 92060I (2014).

[14] V.V. Yashchuk, N.A. Artemiev, I. Lacey, W.R. McKinney, and H.A. Padmore, *Opt. Eng.* **54**(10), 104104 (2015).

[15] http://www.moeller-wedel-optical.com/produkte/elektronische-autokollimatoren/elcomat-3000.html (last accessed 2015-09-02).

[16] R.D. Geckeler, A. Just, M. Krause, and V.V. Yashchuk, *Nucl. Instrum. Methods Phys. Res., Sect. A* **616** 140 (2010).

[17] R.D. Geckeler and A. Just, *Proc. SPIE* **7077**, 70770B (2008).

[18] R.D. Geckeler and A. Just, *Proc. SPIE* **6704**, 670407 (2007).

[19] V.V. Yashchuk, W.R. McKinney, T. Warwick, T. Noll, F. Siewert, T. Zeschke, and R.D. Geckeler, *Proc. SPIE* **6704**, 67040A (2007).

[20] R.D. Geckeler, O. Kranz, A. Just, and M. Krause, *Advanced Optical Technologies* **1**(6), 427 (2012).

[21] S.K. Barber, R.D. Geckeler, V.V. Yashchuk, M.V. Gubarev, J. Buchheim, F. Siewert, and T. Zeschke, *Opt. Eng.* **50**(7), 073602 (2011).

[22] R.D. Geckeler, *Meas. Sci. Technol.* **18**, 115 (2007).

[23] www.anglemetrology.com (EMRP SIB 58 Angle Metrology, last accessed 2015-11-27).

[24] G. Ehret, M. Schulz, A. Fitzenreiter, M. Baier, W. Jockel, M. Stavridis, and C. Elster, *Proc. SPIE* **8082**, 808213 (2011).

[25] A. Just, M. Krause., R. Probst, and R. Wittekopf, *Metrologia* **40**, 288 (2003).

[26] R. Probst, R. Wittekopf, M. Krause, H. Dangschat, and A. Ernst, *Meas. Sci. Technol*. **9**,1059 (1998).

[27] *Evaluation of measurement data – Guide to the expression of uncertainty in measurement* (JCGM 100:2008), http://www.bipm.org/en/publications/guides/gum.html (last accessed 2014-01-28).

[28] A. Just, M. Krause, R. Probst, H. Bosse, H. Haunerdinger, C. Spaeth, G. Metz, and W. Israel, *Precis. Eng.* **33**(4), 530 (2009).

[29] R.D. Geckeler, A. Link, M. Krause, and C. Elster, *Meas. Sci. Technol.* **25**, 055003 (2014).

[30] R.D. Geckeler and A. Just, *Meas. Sci. Technol.* **25**, 105009 (2014).